Optimizing IRE Targeting Using Multi-Electrode Structure and Biomedical Multi-Output Generator

Abstract

Purpose – This paper aims to study the feasibility of proposed method to focus the electroporation ablation by mean of multi-output multi-electrode system.

Design/methodology/approach – The proposed method has been developed based on a previously designed electroporation system, which has the capabilities to modify the electric field distribution in real time, and to estimate the impedance distribution. Taking into consideration the features of the system and biological tissues, the problem has been addressed in three phases: modeling, control system design and simulation testing. In the first phase, a finite element analysis model has been proposed to reproduce the electric field distribution within the hepatic tissue, based on the characteristics of the electroporation system. Then, a control strategy has been proposed with the goal of ensuring complete ablation while minimizing the affected volume of healthy tissue. Finally, to check the feasibility of the proposal, several representative cases have been simulated and the results have been compared with those obtained by a traditional system.

Findings – The proposed method achieves the proposed goal, as part of a complex electroporation system designed to improve the targeting, effectiveness, and control of electroporation treatments and serve to demonstrate the feasibility of developing new electroporation systems capable of adapting to changes in the preplanning of the treatment in real-time.

Originality/value – The work presents a thorough study of control method to multi-output multi-electrode electroporation system by mean of a rigorous numerical simulation.

Keywords – Electroporation, Electric fields, Finite element method, Multi-output .

Paper type – Research paper

1. Introduction

Electroporation (EP) is a phenomenon based on increasing the permeability of cell membranes by means of high intensity electric field that induce strong and short transmembrane potential (Kotnik et al., 2019). Nowadays EP has a wide range of application fields (Kotnik et al., 2015), highlighting biomedical applications(Yarmush et al., 2014). In this context EP can be used to promote or allow the absorption or extraction of drugs or genetic material (Kotnik et al., 2015), increase immune response (Geboers et al., 2020), fuse cells (Geboers et al., 2020), or ablate tissues (Napotnik et al., 2021).

Tissue ablation by EP is currently being used clinically for the treatment of arrhythmias (Sugrue et al., 2018) and tumor destruction (Fang et al., 2021), due to its advantages over thermal treatments such as microwave(Rosin et al., 2018) radiofrequency and cryotherapy. In contrast to thermal treatments, EP ablation allows to ablate tissues with high blood perfusion, preserves their structure(Lopez-Alonso et al., 2019), and can increase the immune response (Zhang et al., 2022), among others advantages which are still being studied.

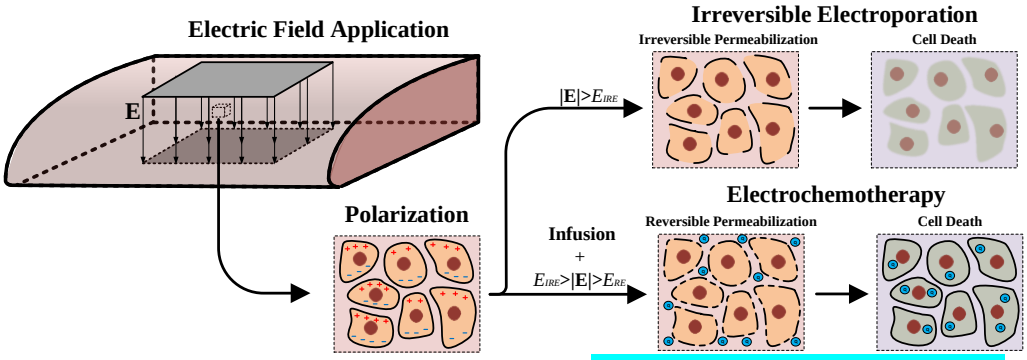

Figure 1. Tissue ablation by electroporation *(Source: Authors' own creation)*

The main EP procedures for tumor treatment are irreversible electroporation (IRE) (Scheffer et al., 2014) and electrochemotherapy (ECT) (Miklavcic et al., 2012, Gothelf et al., 2003, Gehl et al., 2018). In IRE, a high intensity electric field is induced in the tissue, above the irreversible electroporation threshold E_{IRE} (Figure 1). This field is generated by protocols that minimize the power transmitted to the tissue (Davalos et al., 2015) to avoid or minimize thermal effects. The result is an irreversible effect on cell membranes that produces an instantaneous necrosis, or apoptosis or necroptosis (Lopez-Alonso et al., 2019) in the medium term. Then, ECT uses an electric field below the E_{IRE} threshold and above the threshold of reversible electroporation E_{RE} (Figure 1). The result in this case is a temporary increase in the permittivity of cell membranes that allows the uptake of chemotherapeutic drugs such as cisplatin and bleomycin into the cells (Mali et al., 2013), that induces cell death.

Regardless of the EP ablation application the goal is to ensure complete target tissue destruction while preserving healthy tissue as much as possible, which is particularly relevant in tumor ablation to avoid recurrence. Therefore, it is necessary to control the distribution of the electric field within the tissue, and in this way the behavior of the electrical conductivity and the electrodes features have a fundamental role. Moreover, electrical conductivity of biological tissues is heterogeneous, depends on the electric field parameters, and the effects of electroporation (Campana et al., 2019), which makes the targeting of electroporation complex, especially in tumors, which due to the structure the composition and the vascularization may have conductivities several times higher than healthy tissue, measuring tumor tissues with conductivities 5 times higher than surrounded healthy tissue (Marcan et al., 2015).

Standard treatments of IRE ablation an ECT are based on the use of differential electrodes (Malysko-Ptasinske et al., 2023) or electrode arrays (Malysko-Ptasinske et al., 2023) with fixed configurations, since with proper pre-planning of treatments (Zupanic and Miklavcic, 2009) these have proven to be highly effective. However, these electrodes need accurate placement, the volume that can be treated is limited and they are not able to collect much information about the status of the treatment in real time. Moreover, multi-electrodes are structures composed of arrays of electrodes (Lopez-Alonso et al., 2021) in which the voltage applied to each electrode can be controlled independently. This feature allows to perform impedance measurements in different areas to estimate the conductivity distribution (López-Alonso et al., 2022), and it also allows to apply different electric field patterns to control the treated volume (Lopez-Alonso et al., 2021). One handicap of these structures is the complex control system required to process the measurements, and to command the distribution of the applied electric field.

The following section presents a method based on finite element analysis to control a previously designed multi-electrode system (Lopez-Alonso et al., 2023). The aim of this proposal is to obtain the required configurations or activation patterns (APs) of the multi-electrode electroporation system that allows to ensure effective treatment, while minimizing the affected healthy tissue.

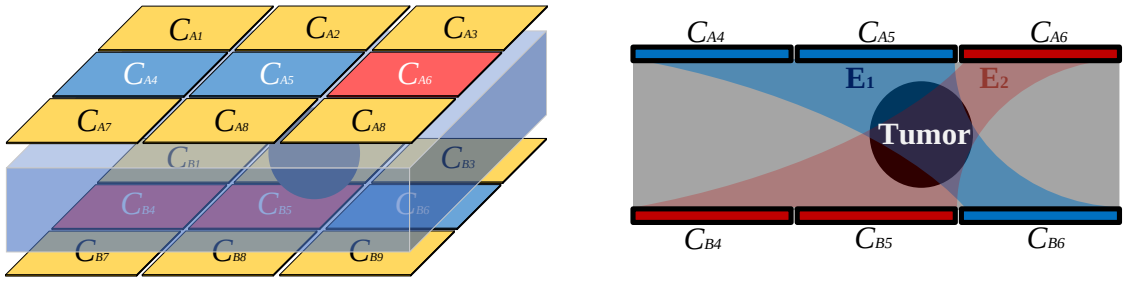

(a) (b)

Figure 2. Electric field application by matrix parallel plate electrode: (a) representation of the electrodes on the tissue with two activation patterns, E1 in blue and E2 in red (b) representation in a cross section of electric field distributions produced by activation patterns E1 (blue) and E2 (red). *(Source: Authors' own creation)*

2. Electric Field Distribution Optimization

Currently, EP tissue ablation is based on the generation of a preplanning electric field pattern between differential electrodes. These electrodes and their positioning are determinant in the distribution of the field in the tissue, and for electroporation the most commonly used are those based on needles or parallel plates.

The electrode family most studied and used in clinical application are needle-based electrodes (Malysko-Ptasinske et al., 2023). These are composed of conductive needles that are generally placed in pairs and must be completely parallel to each other and are used to treat internal and external tumors. These electrodes are easy to position percutaneously, but they concentrate the electric field at the periphery of the needles and show an exponential decay of this field with distance, which limits their separation in order of achieve homogeneous EP avoiding thermal effects. Therefore, these are often used in configurations with more than one pair of needles which can be used to adapt the pattern of the electric field within the (Miklavcic et al., 1998) as well as to increase the treatment volume and the homogeneity and control of the treatment. Moreover, parallel plate based electrodes (Lopez-Alonso et al., 2019) are composed on flat plates that must be placed in parallel in the external part of the tissue to generate a uniform electric field pattern that ideally depends only on the distance between electrodes. Due to their difficult positioning, they are clinically used for the treatment of external tumors, however they create a more uniform electric field than needles that allows the treatment of larger tissue volumes. Also, these do not allow to change the distribution pattern of the electric field without being repositioned. In this line, matrix electrodes based on parallel plates (Lopez-Alonso et al., 2021) have been proposed to work together with a multi-output electroporation generator (Lopez-Alonso et al., 2023) with continuous small-signal impedance monitoring (Pliquett et al., 1995, Ivorra and Rubinsky, 2007, López-Alonso et al., 2020). This system allows impedance mapping to control continuously tissue conductivity changes (Briz et al., 2023) permitting follow the evolution of the treatment, detect problems such as bad contacts and bubbles. Then to improve treatment targeting, with the impedance information it is possible to find the best electric field distribution within the wide range of electric field patterns that the system can generate.

Figure 2 (a) shows a 3D representation of the positioning of the matrix electrodes in a block of healthy tissue with a volume of tumor tissue inside it. As shown in the 2D slice in Figure 2 (b), it is necessary to find the optimal APs to generate an optimal electric field distribution that allows to treat all the tumor tissue, minimizing the volume of healthy tissue electroporated. Among the clinical applications of electroporation, IRE is the one that requires a higher electric field intensity and is the most challenging to optimize in order to achieve a uniform and sure treatment that target the therapeutic effect and minimizes healthy tissue damage. This is since healthy tissue has a lower conductivity, which concentrates the electric field, causing it to be more difficult to reach the necessary intensity in the tumor tissue.

Table I: Electrical Parameters of Non-Biological Materials
(Source: table created by authors)

	σ (s/m)	ξ_r
Steel	3×10^{7}	1
FR4	4×10^{-4}	1

Table II: Electrical Parameters of Biological Tissues (Marcan et al., 2015)
(Source: table created by authors)

	σ_0 (s/m)	σ_f (s/m)	K_v	E_{th} (V/cm)
Liver	4×10^{-2}	1.2×10^{-1}	7.5×10^{-3}	4.75×10^{2}
Tumor	2×10^{-1}	7×10^{-1}	7.5×10^{-3}	6×10^{2}

This section firstly presents the finite element model developed to reproduce the operation of the electroporation system, and then it describes a method to choose the APs. Both the model and the control method have been developed taking into account the capabilities and limitations of the real system such as the capability of the system to estimate the position of tumor tissue volume (Briz et al., 2023).

2.1 Multi-electrode FEA Model

Using COMSOL 6.0 software, two 3D models (Figure 3) have been proposed to carry out the optimization. Parallel flat plate and matrix parallel flat plate geometries are used to perform stationary simulations with the Electric Currents block. The main equations governing the model are first the continuity equation derived from maxwell's laws:

$$\nabla \cdot \mathbf{J} = -\frac{\partial \rho}{\partial t}. \tag{1}$$

It states that the divergence of the current density **J** is equal to the negative of the derivative of the charge density ρ with respect to time. Then **J** is calculated based on ohm's law:

$$\mathbf{J} = \sigma \mathbf{E} + \mathbf{J}_e. \tag{2}$$

where **J** is calculated as the sum of an external current $\mathbf{J_e}$ density and the product of the electric field **E** and the electric conductivity σ. Finally, **E** is calculated as the gradient of the electric potential V:

$$\mathbf{E} = -\nabla V. \tag{3}$$

The electrical potential V is established between the electrodes as the input voltage to the model by means of application patterns.

The models are composed of two types of materials: non-biological materials, biological tissues. The non-biological materials are steel and FR4 (fiberglass-reinforced epoxy resin composite) that are used to build electrodes. Table I lists the electrical parameters of these materials extracted from the COMSOL materials library. The biological tissues considered in the models are liver and tumor (human colorectal liver metastases), and to model the dependence of the conductivity σ on the electric field of biological tissues, the following equation is used:

$$\sigma(|\mathbf{E}|) = (\sigma_0 + \frac{\sigma_f - \sigma_0}{2}(1 + \tanh(K_v(|\mathbf{E}| - E_{th})))) \ , \tag{4}$$

where σ_0 and σ_f are the initial and final electric conductivities of the tissue, respectively. Field E_{th} models the electric field in which the conductivity reaches half of its maximum value. Finally, the constant K_v controls the slope of the curve (Breton et al., 2015). Table II lists the electric parameters used in both tissues.

To perform the analysis, all simulations were carried out using COMSOL 6.0 running on a PC with Windows 10, an Intel I7-7700K processor, and 64 Gb of DDR4 2400 MHz RAM. The mesh size of the models depends on the position of the tumor tissue giving an average of 120000 elements, and a distance between elements between 0.9 mm and 2 mm. Each simulation required an average of 25 sec.

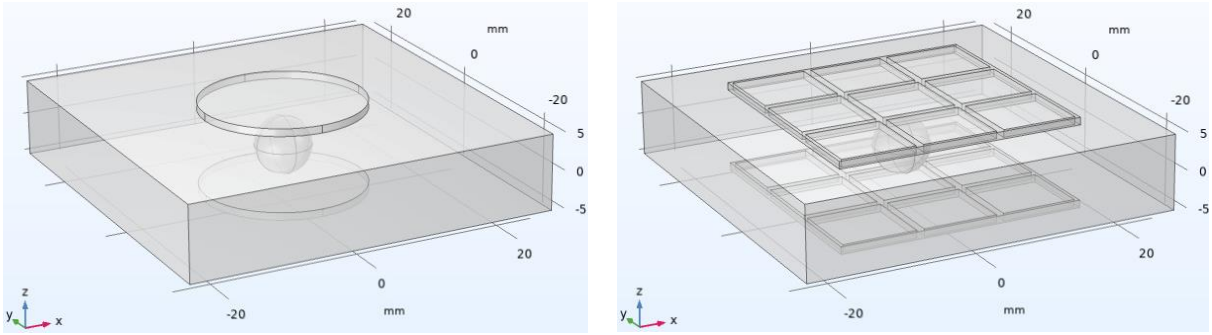

(a) (b)

Figure 3. 3D FEA models geometry: (a) parallel flat plate electrodes (b) matrix parallel flat plate electrodes. *(Source: Authors' own creation)*

Figure 3(a) shows the parallel flat plate geometry, which is used to estimate the minimum voltage needed to treat the tumor volume, and to compare the amount of healthy tissue treated by an ideal parallel flat plate electrode with the results obtained by proposed method. This model is composed of a healthy tissue block with square base of side 5cm and 1cm high, within this block is a sphere of tumor tissue with variable diameter. Finally, there are two cylindrical electrodes with a thickness of 1 mm and variable diameter.

Then, Figure 3(b) shows parallel plate multi-electrode model. This model is used to study the electric field patterns produced in the tissue depending on the APs of the system, and the position and size of the tumor. This model is composed of a healthy tissue block with square base of side 5 cm and 1 cm high, within this block is a sphere of tumor tissue with variable diameter and position. The electrodes are composed of nine square cells of 1 cm side and 1 mm thick, separated by 1 mm of FR4.

Considering the features of the electroporation system (Lopez-Alonso et al., 2023), in the model it is possible to set a voltage difference between the top and bottom electrode, and to select the cells of each electrode connected to this voltage (top electrode) or to ground (bottom electrode). Then, electrode cells that are not active float electrically. The AP of the system defines the active cells of both electrodes.

The model presented is generalist and by adjusting the thresholds and the parameters of the materials it would be possible to use it to evaluate any EP protocol regardless of the shape, number of pulses or any treatment parameter.

2.2 Optimization Method

Each multi-electrode is composed of 9 isolated cells that can be connected to a voltage or left floating. Consequently, each electrode has 2^9 electrode patterns and therefore, the complete system has 2^{18} possible APs. Simulating 2^{18} electric field distributions by means of a finite element model would have a very high computational cost, also, many of the distributions focus the electric field on the healthy tissue. For these reasons, the proposed optimization method has been divided into two phases: firstly, a pre-selection phase of APs capable of affecting the tumor tissue, and a second phase of selection of optimal APs.

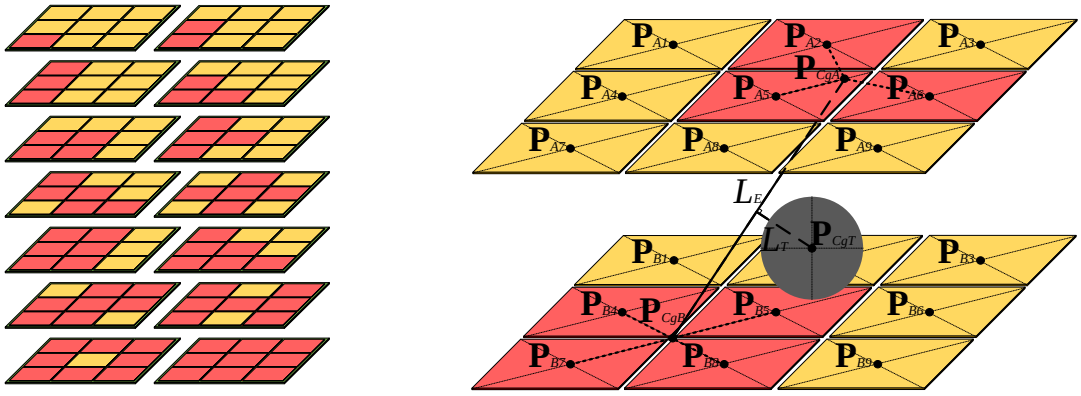

(a) (b)

Figure 4. Representation of electrodes: (a) selected electrode patterns, and(b) graphical calculation of electrode and tumor tissue gravity centers and distances L_E and L_T. *(Source: Authors' own creation)*

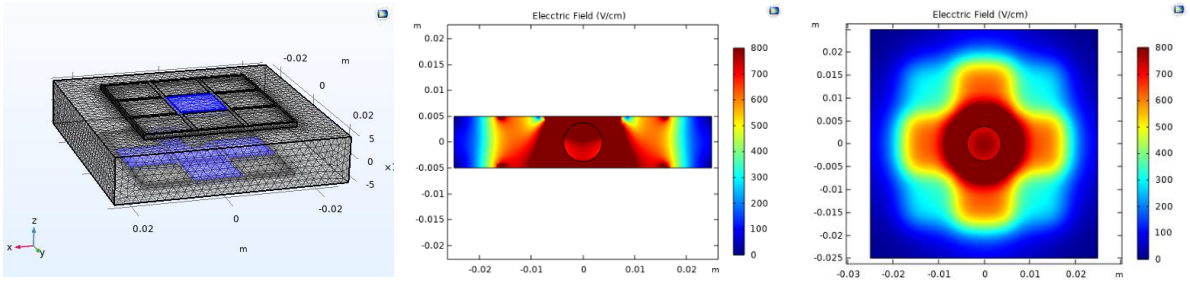

(a) (b) (c)

Figure 5. Simulation of an example of the combination of two APs with a voltage of 1800 V: (a) representation of the APs, (b) electric field distribution in a centered vertical slice and (c) electric field distribution in a centered horizontal slice. *(Source: Authors' own creation)*

The first step of the first phase is to discard all those electrode patterns that are considered chaotic or do not generate a continuous active surface. Figure 4 (a) shows all 14 electrode patterns that have been considered for this optimization, and Figure 5 shows the electric field distribution produced by a combination of the selected APs. Then all these electrode patterns are analyzed in all their possible positions and combinations depending on the position and size of the tumor. As shown in Figure 4 (a), to study the viability of each configuration, first the center of gravity of active electrode cells in top $\mathbf{P}_{CgA}$ and bottom $\mathbf{P}_{CgB}$ electrodes are calculated. The geometric center $\mathbf{P}_{\mathrm{CgN}}$ of N points $\mathbf{P}_n$ is calculated as follows:

$$\mathbf{P}_{CgN} = \frac{1}{N}\left[\sum_{n=1}^{N}\mathbf{P}_n\right]. \tag{5}$$

Then, the distance between the centers of gravity of the two electrodes L_E is calculated. as follows:

$$L_E = |\,\mathbf{P}_{CgA} - \mathbf{P}_{CgB}\,|. \tag{6}$$

Finally, the minimum distance between the vector connecting the centers of gravity of the electrodes L_T with the center of gravity of the tumor tissue is calculated as follows:

$$L_T = \frac{|\,(\mathbf{P}_{CgT} - \mathbf{P}_{CgA}) \times (\mathbf{P}_{CgA} - \mathbf{P}_{CgB})\,|}{|\,(\mathbf{P}_{CgA} - \mathbf{P}_{CgB})\,|}. \tag{7}$$

Two criteria are considered to discard non-useful APs. First, if L_E is greater than 1.5 times the thickness of healthy tissue, it is assumed that it would be necessary to increase the applied voltage to generate an electric field capable of affecting tumor tissue. Secondly, if L_T is greater than half the radius of the tumor, it is assumed that this configuration mainly affects healthy tissue.

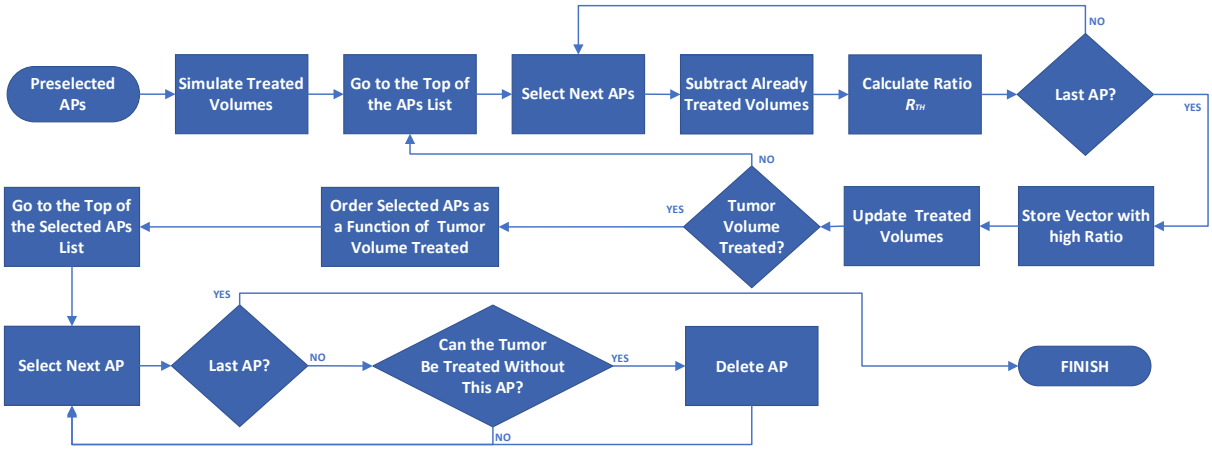

Figure 6. Flow diagram of optimal activation patterns selection process. *(Source: Authors' own creation)*

Figure 6 shows the flow diagram of the second phase. The first step is to find the voltage needed by means of the parallel flat plate model. This voltage is used to simulate by means of the multi-parallel parallel plate model all the APs preselected in the first phase. Next, for each simulated AP, the volume of tumor tissue V_{Tt} that exceeds the irreversible threshold E_{IRE}, and the volume of healthy tissue V_{Ht} that exceeds reversible threshold E_{RE}, are calculated according to the parameters described in (Breton et al., 2015). To evaluate the models, the limits extracted from (Marcan et al., 2015) have used, which are 350 V/cm as E_{RE} for healthy liver tissue and 800 V/cm as E_{IRE} for tumor tissue. With these volumes, the ratio R_{TH} is calculated as:

$$R_{TH} = \frac{V_{Tt}}{V_{Ht}}. \tag{8}$$

The ratio R_{TH} is used to find the AP that maximizes the volume of tumor treated tissue with respect to healthy treated tissue. After choosing the first AP the volume that is treated by this one is subtracted from the remaining simulations, and the ratio R_{TH} is recalculated to find APs until all the tumor tissue volume is treated. The last step of this process is to check if more vectors have been selected than necessary, i.e. if there is any vector whose effect on the tumor tissue can be achieved with the sum of the effects of the others.

The following section presents the results obtained by this procedure in several representative cases.

3. Results

To study the feasibility of the proposal, the performance of the proposed method is analyzed in a practical case and compared with the results of an ideal parallel plate system. The studied case is a spherical tumor of 0.75 cm in diameter placed within continuous healthy tissue of 1 cm thickness.

Using the parallel flat plate model, it has been calculated that the voltage required is 1800 V to achieve in the whole tumor volume an electric field above the E_{IRE} threshold, which has been set at 800 V/cm for all the cases studied. This is achieved if the electrodes are perfectly centered with respect to the tumor, the diameter of the required plates is 2.2 cm. Then, 5 representative positions of the tumor within the tissue were selected.

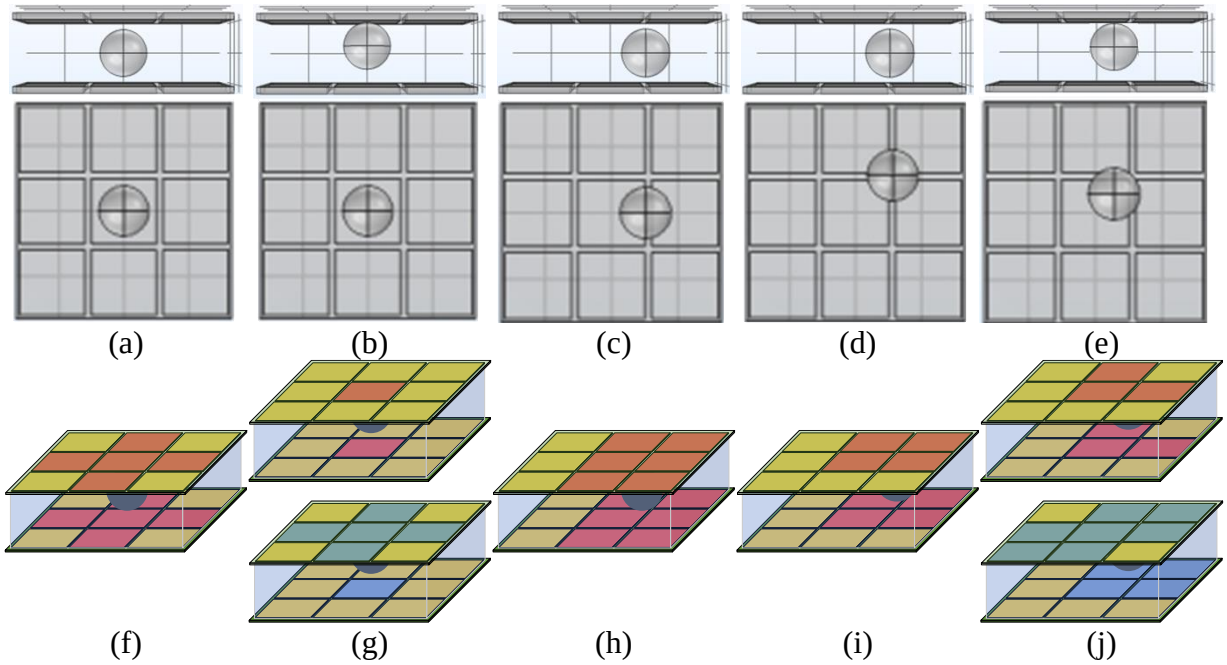

Figure 7. Tumor tissue positions evaluated: (a-e) Case 1-5 (C1-5). Activation patterns obtained for each position: (f-j) APs to the cases C1-5. *(Source: Authors' own creation)*

Table III: Summary of the Results of Cases C1-5 and Ideal Parallel Plate Electrode. *(Source: table created by authors)*

	Preselected APs	Selected APs	Healthy Tissue Treated (cm^3)
C1	444	1	15.37
C2	564	2	9.21
C3	156	1	15.95
C4	107	1	12.9
C5	256	2	14.16
Parallel Plate	-	-	8.82

Figure 7(a-e) shows the 5 positions of the tumor sphere selected, and Figure 7(f-j) shows graphically the APs found for each case. The method has been able to find a combination of PAs to treat the sphere in all the analyzed positions, and Table III summarizes the number of PAs simulated in each case, the final number of PAs needed to treat the sphere in each case and the volume of healthy tissue in which the threshold of reversible electroporation has E_{RE} been overcome.

The following section discusses the results, compares them to traditional parallel plate system, and proposes possible improvements for the studied electroporation system.

4. Discussion

The proposed method achieves the proposed goal, as part of a complex electroporation system designed to improve the targeting, effectiveness, and control of electroporation treatments. However, there are several aspects that deserve to be discussed, such as the direct comparison between the proposed system and a traditional parallel plate electroporation system. In this sense there are two main aspects, versatility, and treatment targeting. In the first aspect, a traditional parallel flat-plate system needs accurate positioning, while the proposed system can adapt to electrode mispositioning, inhomogeneities in the tissue, and is able to treat several masses without the need for repositioning. Moreover, in the focusing aspect, as shown in Table III, in the studied cases the proposed system treats between 4.5 % and 80.8 % more healthy

tissue than parallel plate system. However, this is assuming perfect positioning and an electrode of ideal dimensions, and this is not possible in a real treatment. Therefore, the multi-electrode features could be improved, specifically, by modifying the electrode geometry and the operation of the multi-output generator. The proposed method could reduce the volume of healthy tissue treated. Regarding the geometry the proposed method together with the multi-output generator could be used with any other multi-electrode system based on parallel plates or needles, and specifically in those based on parallel plates, reducing the size of the electrode cells, and increasing their number, which would allow to improve the control of applied electric field distribution. The other aspect that can be enhanced is the operation of the multi-output generator, since the analyzed system only allowed to establish a voltage between the active cells of the top and bottom electrode, leaving the inactive cells floating. Independently controlling the voltage of each electrode cell or connecting the inactive cells to a common point would allow more control over the electric field distribution and therefore increase treatment targeting.

The following is necessary to discuss is the implementation of the proposed method in the complete electroporation system. Considering presented data, the proposed method is not directly implementable in an electroporation system. Due to the number of simulations required, and the average time per simulation with the setup used, it would be necessary to position the electrode and wait in the order of hours to apply the treatment. This handicap can be solved by reducing the simulation time or by carrying out a previous summation. The two strategies proposed to overcome this handicap are the reduction of the simulation time, or to perform a previous simulation phase. To decrease the simulation time, it is necessary to use more powerful computing hardware or to reduce the complexity of the model. Nevertheless, even using both strategies, it is difficult to carry out a minimum of 100 simulations in a time of the order of minutes, without losing too much precision or increasing too much the price of the hardware. Moreover, if the thickness of the tissue and the geometry of the tumor are previously known, it is possible to previously perform the proposed method and find the solutions for the possible positions of the tumor.

Finally, it should be noted that the proposed method along with the electroporation system serve to demonstrate the feasibility of developing new electroporation systems capable of adapting to changes in the preplanning of the treatment and allowing a closed-loop control of the treatment. However, in order to carry out a real application, it would be interesting to design flexible electrodes that could be adapted to all types of tissues and the geometry of their cells and number should be optimized according to the case studied. In addition, the model should also be improved to consider the contact impedances as well as tissues such as skin that can act as an insulator. In this way and for an online application the computational cost of the model should be reduced in order to be able to update it according to changes in the impedance distribution as the treatment progress.

The following section presents the conclusions obtained from this work.

5. Conclusions

Tissue ablation by electroporation shows promising results in the clinical environment, but still has great potential for improvement, especially in the targeting and control of current treatments. The use of multi-electrode structures in combination with multi-output electroporation is one way to improve these aspects. These systems provide a more flexible way to control the electric field distribution and to get more information from the development of the treatments. In this line the proposed method allows to improve the control of these systems to maximize the targeting of treatments and preserve as much healthy tissue as possible regardless of the position of target tissue. The treatment of liver tumors where metastases are common is a field in which the proposed method together with the analyzed electroporation system could be useful locating the different tumors and focusing the treatment on a single application and maximizing the volume of preserved healthy tissue.

Finally, it should be noted that the proposed method along with the electroporation system serve to demonstrate the feasibility of developing new electroporation systems capable of adapting to changes in the preplanning of the treatment and allowing a closed-loop control of the treatment.

Acknowledgements
This work was partly supported by Projects PID2022-136621OB-I00, PDC2021-120898-I00, TED2021-129274B-I00 and ISCIII PI21/00440, co-funded by MCIN/AEI/10.13039/501100011033 and by EU through FEDER and NextGenerationEU/PRTR programs, and by the DGA-FSE, and by Margarita Salas fellowship by the MIU and NextGenerationEU, convocatoria de ayudas para la recualificación del sistema universitario español para 2021-2023, and by DGA under 2021-2025 PhD grant.

References

BRETON, M., BURET, F., KRAHENBUHL, L., LEGUEBE, M., MIR, L. M., PERRUSSEL, R., POIGNARD, C., SCORRETTI, R. & VOYER, D. 2015. Non-Linear Steady-State Electrical Current Modeling for the Electropermeabilization of Biological Tissue. *Ieee Transactions on Magnetics,* 51.

BRIZ, P., LÓPEZ-ALONSO, B., SARNAGO, H., BURDÍO, J. M. & LUCÍA, O. 2023. Tumor location on electroporation therapies by means of multi-electrode structures and machine learning. *Bioelectrochemistry,* 154**,** 108510.

CAMPANA, L. G., DI BARBA, P., DUGHIERO, F., FORZAN, M., MOGNASCHI, M. E., RIZZO, R. & SIENI, E. 2019. Non-parallellism of needles in electroporation: 3D computational model and experimental analysis. *Compel-the International Journal for Computation and Mathematics in Electrical and Electronic Engineering,* 38**,** 348-361.

DAVALOS, R. V., BHONSLE, S. & NEAL, R. E. 2015. Implications and Considerations of Thermal Effects When Applying Irreversible Electroporation Tissue Ablation Therapy. *Prostate,* 75**,** 1114-1118.

FANG, Z., CHEN, L. C., MOSER, M. A. J., ZHANG, W. J., QIN, Z. Y. & ZHANG, B. 2021. Electroporation-Based Therapy for Brain Tumors: A Review. *Journal of Biomechanical Engineering-Transactions of the Asme,* 143.

GEBOERS, B., SCHEFFER, H. J., GRAYBILL, P. M., RUARUS, A. H., NIEUWENHUIZEN, S., PUIJK, R. S., VAN DEN TOL, P. M., DAVALOS, R. V., RUBINSKY, B., DE GRUIJL, T. D., MIKLAVCIC, D. & MEIJERINK, M. R. 2020. High-Voltage Electrical Pulses in Oncology: Irreversible Electroporation, Electrochemotherapy, Gene Electrotransfer, Electrofusion, and Electroimmunotherapy. *Radiology,* 295**,** 254-272.

GEHL, J., SERSA, G., MATTHIESSEN, L. W., MUIR, T., SODEN, D., OCCHINI, A., QUAGLINO, P., CURATOLO, P., CAMPANA, L. G., KUNTE, C., CLOVER, A. J. P., BERTINO, G., FARRICHA, V., ODILI, J., DAHLSTROM, K., BENAZZO, M. & MIR, L. M. 2018. Updated standard operating procedures for electrochemotherapy of cutaneous tumours and skin metastases. *Acta Oncologica,* 57**,** 874-882.

GOTHELF, A., MIR, L. M. & GEHL, J. 2003. Electrochemotherapy: results of cancer treatment using enhanced delivery of bleomycin by electroporation. *Cancer Treatment Reviews,* 29**,** 371-387.

IVORRA, A. & RUBINSKY, B. 2007. In vivo electrical impedance measurements during and after electroporation of rat liver. *Bioelectrochemistry,* 70**,** 287-295.

KOTNIK, T., FREY, W., SACK, M., MEGLIC, S. H., PETERKA, M. & MIKLAVCIC, D. 2015. Electroporation-based applications in biotechnology. *Trends in Biotechnology,* 33**,** 480-488.

KOTNIK, T., REMS, L., TAREK, M. & MIKLAVCIC, D. 2019. Membrane Electroporation and Electropermeabilization: Mechanisms and Models. *In:* DILL, K. A. (ed.) *Annual Review of Biophysics, Vol 48.*

LÓPEZ-ALONSO, B., BRIZ, P., SARNAGO, H., BURDÍO, J. M. & LUCÍA, O. 2022. Real-Time Conductivity Distribution Characterization for Electroporation using Plant Tissue *4º World congress on electroporation and pulsed electric fields in biology, medicine,*

food and environmental thechnologies. Copenhagen, Denmark: The International Society for Electroporation-Based Technologies and Treatments (ISEBTT).

LOPEZ-ALONSO, B., HERNAEZ, A., SARNAGO, H., NAVAL, A., GUEMES, A., JUNQUERA, C., BURDIO, J. M., CASTIELLA, T., MONLEON, E., GRACIA-LLANES, J., BURDIO, F., MEJIA, E. & LUCIA, O. 2019. Histopathological and Ultrastructural Changes after Electroporation in Pig Liver Using Parallel-Plate Electrodes and High-Performance Generator. *Scientific Reports,* 9.

LOPEZ-ALONSO, B., SARNAGO, H., BURDIO, J. M., BRIZ, P. & LUCIA, O. 2021. Multi-Electrode Architecture Modeling and Optimization for Homogeneous Electroporation of Large Volumes of Tissue. *Energies,* 14.

LOPEZ-ALONSO, B., SARNAGO, H., BURDIO, J. M. & LUCIA, O. 2023. Multiple Output Inverter and Monitoring System for Homogeneous Electroporation. *Ieee Transactions on Power Electronics,* 38**,** 1935-1947.

LÓPEZ-ALONSO, B., SARNAGO, H., LUCÍA, O., BRIZ, P. & BURDÍO, J. M. 2020. Real-Time Impedance Monitoring During Electroporation Processes in Vegetal Tissue Using a High-Performance Generator. *Sensors,* 20.

MALI, B., JARM, T., SNOJ, M., SERSA, G. & MIKLAVCIC, D. 2013. Antitumor effectiveness of electrochemotherapy: A systematic review and meta-analysis. *Ejso,* 39**,** 4-16.

MALYSKO-PTASINSKE, V., STAIGVILA, G. & NOVICKIJ, V. 2023. Invasive and non-invasive electrodes for successful drug and gene delivery in electroporation-based treatments. *Frontiers in Bioengineering and Biotechnology,* 10.

MARCAN, M., KOS, B. & MIKLAVCIC, D. 2015. Effect of Blood Vessel Segmentation on the Outcome of Electroporation-Based Treatments of Liver Tumors. *Plos One,* 10.

MIKLAVCIC, D., BERAVS, K., SEMROV, D., CEMAZAR, M., DEMSAR, F. & SERSA, G. 1998. The importance of electric field distribution for effective in vivo electroporation of tissues. *Biophysical Journal,* 74**,** 2152-2158.

MIKLAVCIC, D., SERSA, G., BRECELJ, E., GEHL, J., SODEN, D., BIANCHI, G., RUGGIERI, P., ROSSI, C. R., CAMPANA, L. G. & JARM, T. 2012. Electrochemotherapy: technological advancements for efficient electroporation-based treatment of internal tumors. *Medical & Biological Engineering & Computing,* 50**,** 1213-1225.

NAPOTNIK, T. B., POLAJZER, T. & MIKLAVCIC, D. 2021. Cell death due to electroporation - A review. *Bioelectrochemistry,* 141.

PLIQUETT, U., LANGER, R. & WEAVER, J. C. 1995. Changes in the passive electrical properties of human stratum corneum due to electroporation. *Biochimica et Biophysica Acta (BBA) - Biomembranes,* 1239**,** 111-121.

ROSIN, A., HADER, M., DRESCHER, C., SUNTINGER, M., GERDES, T., WILLERT-PORADA, M., GAIPL, U. S. & FREY, B. 2018. Comparative study and simulation of tumor cell inactivation by microwave and conventional heating. *Compel-the International Journal for Computation and Mathematics in Electrical and Electronic Engineering,* 37**,** 1893-1904.

SCHEFFER, H. J., NIELSEN, K., DE JONG, M. C., VAN TILBORG, A., VIEVEEN, J. M., BOUWMAN, A. R. A., MEIJER, S., VAN KUIJK, C., VAN DEN TOL, P. M. P. & MEIJERINK, M. R. 2014. Irreversible Electroporation for Nonthermal Tumor Ablation in the Clinical Setting: A Systematic Review of Safety and Efficacy. *Journal of Vascular and Interventional Radiology,* 25**,** 997-1011.

SUGRUE, A., MAOR, E., IVORRA, A., VAIDYA, V., WITT, C., KAPA, S. & ASIRVATHAM, S. 2018. Irreversible electroporation for the treatment of cardiac arrhythmias. *Expert Review of Cardiovascular Therapy,* 16**,** 349-360.

YARMUSH, M. L., GOLBERG, A., SERSA, G., KOTNIK, T. & MIKLAVCIC, D. 2014. Electroporation-Based Technologies for Medicine: Principles, Applications, and Challenges. *In:* YARMUSH, M. L. (ed.) *Annual Review of Biomedical Engineering, Vol 16.*

ZHANG, N. A., LI, Z. Q., HAN, X., ZHU, Z. Y., LI, Z. J., ZHAO, Y., LIU, Z. J. & LV, Y. 2022. Irreversible Electroporation: An Emerging Immunomodulatory Therapy on Solid Tumors. *Frontiers in Immunology,* 12.

ZUPANIC, A. & MIKLAVCIC, D. 2009. Method for treatment planning of tissue ablation by irreversible electroporation. 11th International Congress of the IUPESM/World Congress on Medical Physics and Biomedical Engineering, Sep 07-12 2009 Munich, GERMANY. 150-153.